

Influence of Fiber Content on Properties of Oil Palm Mesocarp Fiber/Poly(butylene succinate) Biocomposites

Yoon Yee Then,^a Nor Azowa Ibrahim,^{a,*} Norhazlin Zainuddin,^a Hidayah Ariffin,^b Buong Woei Chieng,^a and Wan Md Zin Wan Yunus^c

Biodegradable and environmentally friendly biocomposites produced by a combination of biodegradable thermoplastics and natural fiber have gained increasing interest in recent years. In this work, eco-friendly biocomposites made from poly(butylene succinate) (PBS) and different weight percentages (10, 30, 50, and 70 wt%) of oil palm mesocarp fiber (OPMF) were fabricated *via* a melt blending process followed by hot-press molding. The biocomposites showed an improvement in storage and loss moduli with increasing fiber content, as indicated by dynamic mechanical analysis. Also, the water uptake and thickness swelling of the biocomposites increased with fiber content. The presence of fiber improved the biodegradability of the PBS, as evidenced from soil decomposition and scanning electron microscopy studies. Conversely, the presence of fiber lowered the melting and crystallization temperature as well as the thermal stability of neat PBS. The biocomposites from PBS and OPMF could be promising biocomposite materials because of their improved mechanical properties and biodegradability compared to neat PBS.

Keywords: Biodegradability; Dynamic mechanical analysis; Oil palm mesocarp fiber; Poly(butylene succinate); Thermal; Dimensional stability

Contact information: a: Department of Chemistry, Faculty of Science, Universiti Putra Malaysia, 43400 UPM Serdang, Selangor, Malaysia; b: Department of Bioprocess Technology, Faculty of Biotechnology and Biomolecular Sciences, Universiti Putra Malaysia, 43400 UPM Serdang, Selangor, Malaysia; c: Department of Chemistry, Centre For Defence Foundation Studies, National Defence University of Malaysia, Sungai Besi Camp, 57000 Kuala Lumpur, Federal Territory of Kuala Lumpur, Malaysia; * Corresponding author: norazowa@upm.edu.my

INTRODUCTION

Eco-friendly biocomposites from natural fibers and bio-based biodegradable thermoplastics are of great importance, as they provide a feasible solution to recently growing environmental threats as well as a sustainable solution to replace thermoplastics or composites derived from limited petrochemical resources (Mohanty *et al.* 2002).

Natural fibers possess several advantages over synthetic fibers, such as low cost and low density, biodegradability, eco-friendliness, renewability, and high specific strength and stiffness relative to synthetic fibers (Terzopoulou *et al.* 2014). Furthermore, natural fiber can be obtained at a relatively low energy input with a lesser amount of CO₂ emissions; they cause little abrasion to machinery during processing compared to synthetic fibers (Azizi Samir *et al.* 2005).

According to recent publications, a wide range of natural fibers are being utilized as filler or reinforcement in various types of thermoplastic matrices to fabricate biocomposites; these include oil palm (Shinoj *et al.* 2010, 2011a,b; Teh *et al.* 2013; Eng *et al.* 2014; Rayung *et al.* 2014; Then *et al.* 2013, 2014a, 2015a,b), kenaf (Abdul Razak *et al.* 2014), hemp (Terzopoulou *et al.* 2014), jute (Nam *et al.* 2012), coir (Nam *et al.* 2011), cotton stalk (Tan *et al.* 2011), sisal (Joseph *et al.* 2003), and banana (Pothan *et al.* 2003).

Malaysia is currently the largest palm oil exporter in the world, and the second largest palm oil producer after Indonesia. Consequently, large quantities of oil palm biomass are produced in either the plantation area or oil palm mills. Among biomass, oil palm mesocarp fiber (OPMF) is of interest here. OPMF is available in large quantities at palm oil mills after extraction of crude palm oil from the oil palm fruits (Sreekala *et al.* 1997). It can be obtained at almost zero cost, as it is considered a waste and no extra processing aid is needed for obtaining the fiber. It has been traditionally used as a low value boiler fuel to produce steam in generating electricity for self-supply in oil palm mills. In the authors' previous reports (Teh *et al.* 2013; Eng *et al.* 2014; Then *et al.* 2013, 2014a, 2015a,b), OPMF was successfully compounded with biodegradable thermoplastics to produce eco-friendly biocomposites. This undoubtedly will be an added value of OPMF in the future.

Poly(butylene succinate) (PBS), a biodegradable thermoplastic, was chosen to be used in this work due to its low market price relative to other biodegradable thermoplastics as well as its processability under low temperatures (~120 °C), which would not degrade OPMF during the compounding process (Nam *et al.* 2011). The mechanical properties of PBS are reportedly similar to those of conventional thermoplastics such as polyethylene and polypropylene, which are derived from petroleum and non-biodegradable sources (Nam *et al.* 2012). Further, PBS is a sustainable thermoplastic as it can be produced from bio-based derived monomers of succinic acid and 1, 4-butanediol *via* a poly-condensation reaction (Xu and Guo 2010).

Dynamic mechanical analysis has been widely used to study the interfacial properties of biocomposite materials. It provides information regarding the visco-elastic behavior of the corresponding biocomposites in terms of storage and loss moduli, as well as loss factor. Joseph *et al.* (2003) studied the dynamic mechanical properties of short sisal fiber reinforced polypropylene composites. They reported that the storage modulus of the composite was increased with increasing weight percentage of fiber. Apart from that, crystallization behavior of the biocomposite, which can be studied by means of differential scanning calorimetry, is also important as it can influence the biodegradability of the corresponding biocomposites, as well as their mechanical and thermal properties (Bikiaris *et al.* 2006). In the meantime, the information regarding the moisture content and thermal breakdown of the biocomposites can be obtained by using thermogravimetric analysis (Kim *et al.* 2005a).

In the previous work (Then *et al.* 2013), the authors succeeded in producing biocomposites from PBS and OPMF, and their mechanical properties including tensile, flexural, and ability to take an impact were reported. Apart from mechanical properties, the thermal properties, biodegradability, and dimensional stability of the biocomposite are also important for their processing and application as are disposal after the shelf life expires. Hence, the dynamic mechanical and thermal properties, biodegradability, and dimensional stability of OPMF/PBS biocomposites are reported in this paper.

EXPERIMENTAL

Materials

Oil palm mesocarp fiber (OPMF) was collected from FELDA Seriting Hilir Oil Palm Mill, Jempol, Malaysia. It was first washed by soaking in distilled water at 25 °C for 24 h, then rinsed with hot water (60 °C) followed by acetone prior to oven-drying at 60 °C. This process was carried out to remove dirt adhered to the fibers' surface as well as some oil residues. The dried fiber was then ground and sieved to obtain particles with sizes between 150 to 300 µm for use in biocomposite preparation. The properties of OPMF can be found in the authors' previous work (Then *et al.* 2014b). Poly(butylene succinate) (PBS), under the trade name of BIONOLLE™ 1903MD, was purchased from Showa Denko, Tokyo, Japan. It has a density of 1.26 g/cm³ and melting point of ~115 °C. Its repeating unit is shown in Fig. 1.

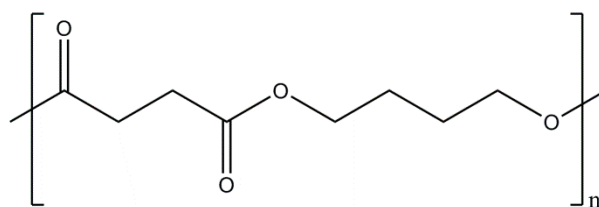


Fig. 1. Repeating unit of PBS

Methods

Fabrication of OPMF/PBS biocomposites

Both OPMF and PBS were oven-dried at 60 °C prior to compounding. Dried materials were weighed separately according to the proportion as shown in Table 1. The pre-weighed materials were then manually fed into a Brabender internal mixer at a temperature of 120 °C and 50 rpm rotor speed. In brief, PBS pellets were first fed into the mixing chamber to melt for 2 min. After that, OPMF was added to the molten PBS and mixing continued for a total time of 15 min. The compounded materials were then hot-press molded into sheets of 1 mm thickness at 120 °C with a pressing pressure of 14.71 MPa for 5 min and cooled at 30 °C for 5 min.

Table 1. Proportion of OPMF and PBS

Sample code	PBS (wt%)	OPMF (wt%)
PBS	100	0
10 OPMF/PBS	90	10
30 OPMF/PBS	70	30
50 OPMF/PBS	50	50
70 OPMF/PBS	30	70
OPMF	0	100

Fourier transform infrared (FTIR) spectroscopy

The functional groups and types of bonding in PBS, OPMF, and their biocomposites were identified using a Perkin Elmer Spectrum 100 series spectrophotometer equipped with attenuated total reflectance (ATR). The FTIR spectra of the samples were recorded over the range of frequencies from 400 to 4000 cm⁻¹.

Dynamic mechanical analysis (DMA)

Dynamic mechanical properties of PBS and its biocomposites were examined according to the American Society of Testing and Materials (ASTM) D5023 standard (ASTM 2009), using a Perkin-Elmer PYRIS Diamond dynamic mechanical analyzer with bending mode. The dimensions of the specimens used were 40 mm in length, 13 mm in width, and 1 mm thick. The temperature scan was from -80 to 50 °C at a constant heating rate of 10 °C/min with the frequency of dynamic force of 1 Hz, under a nitrogen atmosphere. The storage modulus (E'), loss modulus (E''), and damping properties ($\tan \delta$) of each specimen were recorded as a function of temperature.

Differential scanning calorimetric (DSC) analysis

Melting and crystallization behaviors of the PBS and its biocomposites were studied using a differential scanning calorimeter according to the ASTM D3418 standard (ASTM 2008). The weight of the sample used was around 8 to 10 mg. The samples were first heated from 60 to 130 °C with the heating rate of 10 °C/min and kept at this temperature for 3 min to remove the thermal history of the samples. The samples were then cooled down to 60 °C with the cooling rate of 10 °C/min, to allow the samples to crystallize dynamically, and kept at this temperature for 3 min. Subsequently, the crystallized samples were then re-heated up to 130 °C with the heating rate of 10 °C/min. All the heating and cooling scans run in melting and crystallization studies were carried out under a nitrogen (N_2) atmosphere at a flow rate of 20 mL/min to prevent oxidation of the samples. The degree of crystallinity, or crystallinity index (χ_c), was determined from the second melting enthalpy values using the following (Eq. 1),

$$\chi_c = \frac{\Delta H_m}{\alpha \Delta H_m^0} \times 100 \quad (1)$$

where ΔH_m is the melting enthalpy of the samples (J/g), ΔH_m^0 is the enthalpy value of melting of a 100% crystalline form of poly(butylene succinate) (110.3 J/g), and α is the weight fraction of thermoplastics in the biocomposite materials.

Thermogravimetric analysis (TGA)

Thermal degradation behaviors of OPMF, PBS, and their biocomposites were studied using a Perkin Elmer Pyris 7 TGA analyzer with a temperature range of 35 to 500 °C at a constant heating rate of 10 °C/min and continuous nitrogen flow of 20 mL/min. The weights of the samples used were from 10 to 15 mg. The weight losses of samples were recorded as a function of temperature.

Dimensional stability

The dimensional stability of PBS and its biocomposites was assessed *via* water absorption and thickness swelling tests; these were conducted according to the ASTM D570 standard (2005) and European EN 317 (2003) standard, respectively. Samples with the dimensions 10.0 mm by 10.0 mm by 1.0 mm were cut from the 1 mm sample sheets and used for testing. The samples were oven-dried at 60 °C until a constant weight was reached prior to testing. The initial weight (W_0) and thickness (T_0) of the dried samples were measured using a microbalance and caliper, respectively. The samples were then immersed in distilled water for 24 h at 25 °C. After that, the samples were removed from the distilled water and wiped with tissue paper to remove excess water on their surfaces.

The final weight (W_{24h}) and thickness (T_{24h}) of the samples were measured immediately. The tests were performed in duplicate, and the average values and standard deviations were reported. The water absorption as well as the thickness swelling of the biocomposites was calculated following Eqs. 2 and 3, respectively:

$$\text{Water Absorption (\%)} = \frac{W_{24h} - W_0}{W_0} \times 100 \quad (2)$$

$$\text{Thickness Swelling (\%)} = \frac{T_{24h} - T_0}{T_0} \times 100 \quad (3)$$

Biodegradation test

The biodegradability of PBS and its biocomposites was studied using the natural soil burial test as described by Kim *et al.* (2005b). The specimens were cut into pieces measuring 10 mm by 10 mm by 1 mm and used for testing. The specimens were dried in an oven at 60 °C for 24 h prior to testing. The initial weight of specimens (W_i) was recorded using a microbalance with accuracy of ± 0.0001 g. The specimens were then buried in a box containing natural soil (obtained from Universiti Putra Malaysia) at 25 °C. The specimens were buried at a depth of 8 cm, and water was supplied every three days to keep the soil in a moist condition. The specimens were taken out once every month for a period of five months, washed with distilled water, dried in an oven at 60 °C for 48 h; this was followed by equilibration in a desiccator for 24 h. The specimens were then weighed to obtain the final weight (W_f). The percentage weight loss was taken from the average of three specimens and calculated based on Eq. 4.

$$\text{Weight Loss (\%)} = \frac{W_i - W_f}{W_i} \times 100 \quad (4)$$

Scanning electron microscopy (SEM)

The morphologies of soil buried-degraded PBS and its biocomposites were examined using a JEOL JSM-6400 scanning electron microscope operated at an accelerated voltage of 15 kV. The surfaces of specimens were sputter-coated with gold prior to analysis in order to prevent electrical discharge.

RESULTS AND DISCUSSION

Fourier Transform Infrared (FTIR) Spectroscopy

The FTIR spectra of OPMF, PBS, and OPMF/PBS biocomposites of various weight percentages OPMF content are elucidated in Fig. 2.

The characteristic peaks of PBS can be found at 2949, 1715, and 1170 cm^{-1} , corresponding to C-H stretching, C=O stretching, and C-O-C stretching, respectively (Zhao *et al.* 2010). Meanwhile, the absorption peaks of OPMF appeared at 3391 cm^{-1} , and the peaks at 2925 and 2853, 1730, and 1645 cm^{-1} were attributed to O-H stretching in the cellulose, water and lignin, C-H stretching present in the cellulose and hemicellulose, C=O stretching in hemicellulose, and O-H bending of the absorbed water, respectively (Then *et al.* 2014b).

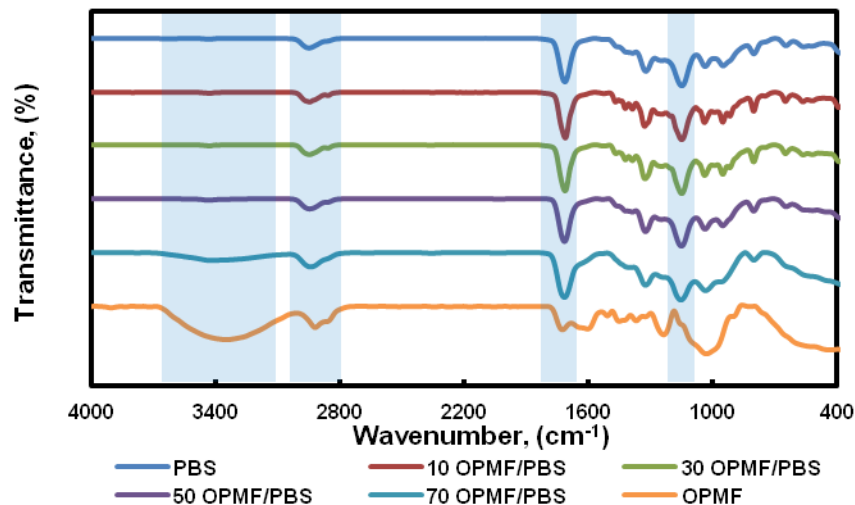


Fig. 2. FTIR spectra of neat PBS, OPMF, and biocomposites of various OPMF content

It was apparent that the absorption peaks in the spectra of OPMF/PBS biocomposites were a combination of absorption peaks between PBS and OPMF, as no new peak was formed. Furthermore, the O-H stretching peak for the biocomposites appeared to be intensified as the fiber content increased. This is probably explained by the hydroxyl groups that are present in fiber. Moreover, a weak absorption band was also noted at 1645 cm^{-1} in the spectra of biocomposites, especially on the biocomposite with higher OPMF content, originating from the O-H bending of the absorbed water. Those results signified that OPMF/PBS biocomposites became relatively more hydrophilic than that of neat PBS, which is in accordance with the results of the water absorption test (as discussed in a later section).

Dynamic Mechanical Analysis

Biocomposite materials can be subjected to various types of dynamic stressing during use; therefore studies of their thermo-mechanical behavior to determine their relevant stiffness and damping characteristics for diverse applications are of great importance (Joseph *et al.* 2003). Figure 3 depicts the storage modulus (E') as a function of temperature for the neat PBS and its biocomposites. The E' is denoted as the elastic part of the material and thus describes the ability of the material to bear a load. A high E' indicates a more rigid material.

It is clear from Fig. 3 that the E' of neat PBS and OPMF/PBS biocomposites decreased with increasing temperature. This is related to the softening and increased chain mobility of PBS at higher temperatures (Kim *et al.* 2005a). Generally, the E' of OPMF/PBS biocomposites was higher relative to that of neat PBS over the entire temperature range and increased with increasing of fiber content up to 70 wt%. The initial introduction of OPMF at 10 and 30 wt% only marginally increased the E' , and then it increased drastically at 50 and 70 wt% of OPMF. This is attributed to the reinforcement imparted by the OPMF that allows greater stress transfer at the interface from the PBS to OPMF (Kim *et al.* 2005a). A similar trend was observed by Joseph *et al.* (2003) in their work related to short sisal fiber reinforced polypropylene composites. This result also implied that the stiffness of the biocomposites was considerably improved in comparison to that of the neat PBS.

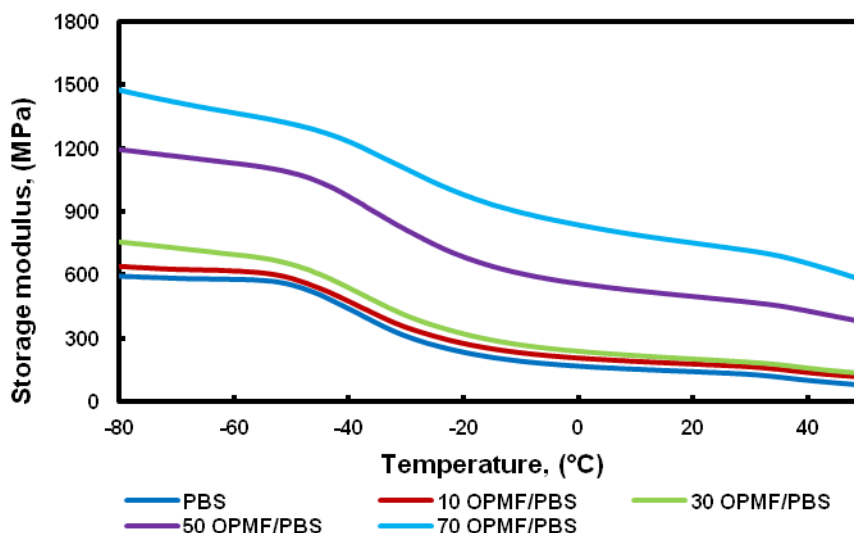


Fig. 3. Storage modulus of neat PBS and biocomposites of various OPMF content

As temperatures further increased to around $-50\text{ }^{\circ}\text{C}$, a dramatic drop in E' could be seen at all curves, which was related to the phase transition of the materials from the rigid glassy state where molecular motions are restricted to a more flexible rubbery state where the molecular chains have greater mobility (Rezaei *et al.* 2009). After that, the E' continued to drop gradually due to the further increased chain mobility of PBS at higher temperature (Kim *et al.* 2005a). It was apparent that the drop in E' from the glassy to rubbery state was relatively less for OPMF/PBS biocomposites than for that of neat PBS, and this effect became more prominent at higher OPMF contents. This can be explained by the mechanical restraint produced by the fiber, which can reduce the mobility and deformability of the PBS during the phase transition region (Pothan *et al.* 2003).

Table 2. Storage Modulus (E'), Loss Modulus (E''), and Glass Transition Temperature (T_g) of PBS and Its Biocomposites

Sample	E' at $-60\text{ }^{\circ}\text{C}$ (MPa)	E' at $30\text{ }^{\circ}\text{C}$ (MPa)	E'' at maximum peak height (MPa)	T_g ($^{\circ}\text{C}$)
PBS	579	128	488	-33.16
10 OPMF/PBS	618	164	519	-32.96
30 OPMF/PBS	697	186	567	-31.49
50 OPMF/PBS	1131	472	733	-30.64
70 OPMF/PBS	1366	711	1032	-28.57

For comparison, the E' of PBS and its biocomposites at temperatures of -60 (glassy state) and $30\text{ }^{\circ}\text{C}$ (rubbery state) are tabulated in Table 2. It was evident from the table that the E' at $-60\text{ }^{\circ}\text{C}$ was substantially higher than that of E' at $30\text{ }^{\circ}\text{C}$ for both neat PBS and its biocomposites. This signifies that molecules in the glassy state had higher E' than did molecules in the rubbery state, *i.e.*, the E' of 70 OPMF/PBS biocomposite was 1366 and 711 MPa for -60 and $30\text{ }^{\circ}\text{C}$, respectively. Additionally, the E' of OPMF/PBS biocomposites at a particular temperature was relatively higher than that of neat PBS. This implies that the introduction of OPMF into PBS increased the E' of the biocomposites, and this effect was more prominent for biocomposites with higher fiber content. It was noted that at $30\text{ }^{\circ}\text{C}$, the E' of PBS was 128 MPa, and this value increased

to 711 MPa for biocomposites with 70 wt% OPMF, showing a 455% increase. This result is in line with the tensile and flexural moduli measurements reported previously (Then *et al.* 2013). The increase in E' can be explained by the fact that the presence of OPMF restricted the chain mobility of PBS, thereby stiffening the biocomposite and resulting in a higher E' . A similar observation was also reported by Tan *et al.* (2011) in poly(butylene succinate) composites reinforced with cotton stalk bast fibers.

Figure 4 shows the temperature dependence of the loss modulus (E'') for PBS and OPMF/PBS biocomposites of different OPMF weight percentages. The E'' is equivalent to the dissipated energy, and the peak height of loss modulus curves signifies the melt viscosity of a material (Rezaei *et al.* 2009). As can be seen in Fig. 4, the E'' followed the same trend as that of E' . It was apparent that with an increase in temperature, the E'' curves of neat PBS, as well as its biocomposites, reached a maximum peak height and thereafter decreased. This is attributed to the maximum dissipation of energy caused by the free movement of the PBS chains. As shown in Table 2, the OPMF/PBS biocomposites showed higher E'' relative to that of PBS at all fiber loadings. This indicated that a higher melt viscosity was achieved as a result of the molecular movement restriction due to the presence of the fiber (Rezaei *et al.* 2009). Among the biocomposites, a higher peak height for E'' was noted with higher OPMF content. This is attributed to the increased contact and friction between OPMF and PBS at higher fiber contents, as energy was dissipated by the friction between OPMF and PBS at the interface region and consequently led to relatively high E'' .

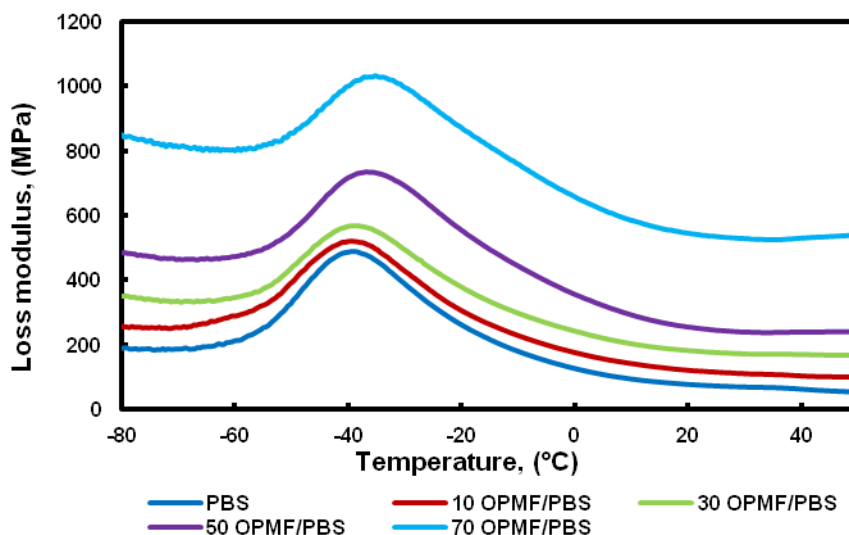


Fig. 4. Loss modulus of neat PBS and its biocomposites of various OPMF content

Figure 5 shows the variation of $\tan \delta$ as a function of temperature for neat PBS and its biocomposites. $\tan \delta$ is taken as the ratio of E'' to E' , reflecting the damping properties of the material. The height of the peak for the OPMF/PBS biocomposites appeared to be lower in comparison to that of neat PBS and become more prominent at higher content of OPMF as illustrated in Fig. 5, reflecting a decrease in damping property of PBS by the presence of OPMF. At the same time, a broadening of the $\tan \delta$ peak was also seen as the content of OPMF was increased. A broader peak indicated more time for relaxation of molecules due to lower polymeric chain movement resulting from mobility restriction by fiber in the biocomposites (Harris *et al.* 1993). In addition, the maximum peak of $\tan \delta$, which is commonly known as the glass transition temperature (T_g) of

OPMF/PBS biocomposites, appeared to be shifted toward higher temperature in comparison to that of neat PBS as evidenced by a shift of the maximum peak to the right. The shifting magnitude of $\tan \delta$ peak was greater at higher OPMF content, *i.e.*, the T_g of neat PBS was found to be -33.16°C and shifted to higher temperatures of -32.96 , -31.49 , -30.64 , and -28.57°C for biocomposites of 10, 30, 50, and 70 wt% OPMF, respectively. The shifting of T_g in the biocomposites to higher temperatures results from decreased mobility of the polymer chains due to the presence of fiber (Pothan *et al.* 2003).

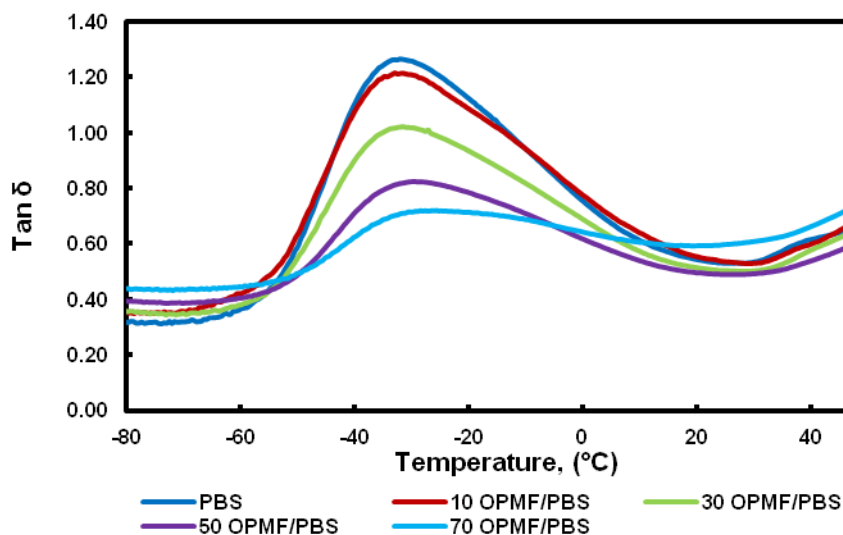


Fig. 5. Loss factor of neat PBS and its biocomposites of various OPMF content

Differential Scanning Calorimetric (DSC) Analysis

The DSC heating and cooling thermograms of neat PBS and OPMF/PBS biocomposites of 10, 30, 50, and 70 wt% OPMF are presented in Figs. 6 and 7, respectively.

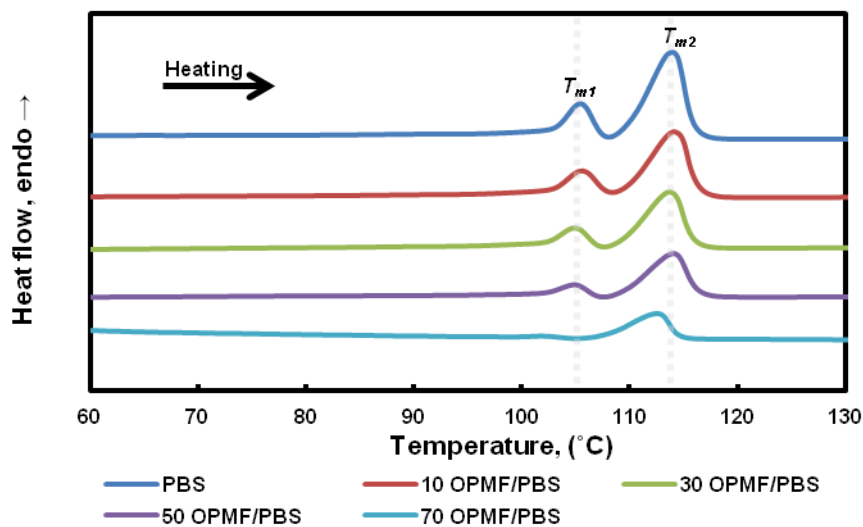


Fig. 6. DSC heating thermograms of neat PBS and its biocomposites of various OPMF content

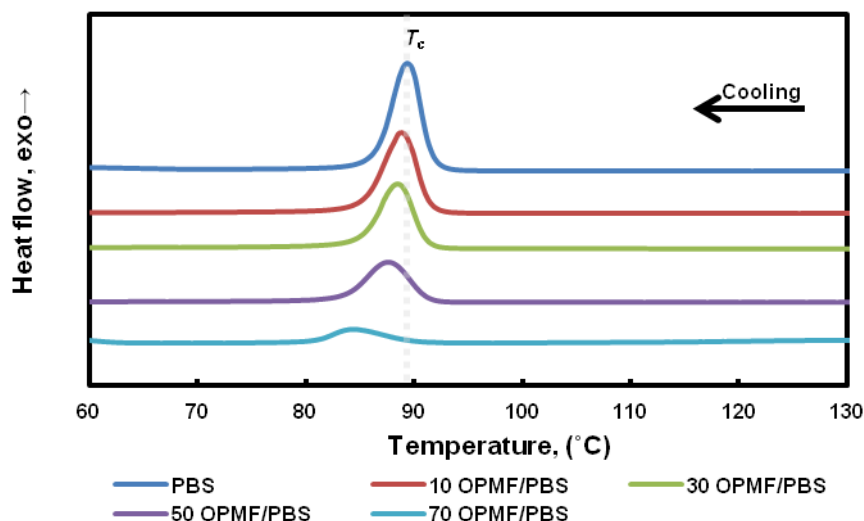


Fig. 7. DSC cooling thermograms of neat PBS and its biocomposites of various OPMF content

Their first melting temperature (T_{m1}), second melting temperature (T_{m2}), melting enthalpy (ΔH_m), crystallization temperature (T_c), crystallization enthalpy (ΔH_c) and crystallinity (χ_c) were determined from their DSC thermograms and tabulated in Table 3. The T_{m1} , T_{m2} , ΔH_m (area under the T_{m2}), and χ_c were taken and calculated from the second heating scan while the T_c and ΔH_c (area under the T_c) were obtained from the first cooling scan.

As can be seen in Fig. 6, the DSC heating thermogram of neat PBS showed two endothermic peaks due to the melting and re-crystallization mechanism (Yasuniwa and Satou 2002). The first melting peak was ascribed to the melting of less perfect crystals. The re-crystallization process occurred immediately after the first melting as indicated by the presence of a small exothermic peak right after the first endothermic peak. As the temperature increased, the re-crystallized or more structurally perfect crystal melted and gave rise to the second melting endothermic peak (Zhang *et al.* 2012). A similar observation was reported by Terzopoulou *et al.* (2014) for hemp/PBS biocomposites. During the cooling scan, the DSC thermogram (Fig. 7) of neat PBS showed the presence of an exothermic peak. This peak is related to the crystallization of PBS from the molten stage upon cooling.

Table 3. Melting Temperature, Enthalpy of Melting, Crystallization Temperature, Enthalpy of Crystallization, and Crystallinity of PBS and its Biocomposites

Sample	T_{m1} (°C)	T_{m2} (°C)	ΔH_m (J/g)	T_c (°C)	ΔH_c (J/g)	χ_c (%)
PBS	104.7	113.4	57.7	89.5	68.2	52.3
10 OPMF/PBS	104.7	113.3	49.1	89.1	57.9	49.4
30 OPMF/PBS	104.1	113.1	36.2	88.6	47.1	46.9
50 OPMF/PBS	104.1	113.4	22.3	87.7	35.6	40.3
70 OPMF/PBS	101.0	111.9	10.9	84.9	18.6	32.9

In general, two endothermic peaks (heating scan) and one exothermic peak (cooling scan) were present in the DSC thermograms of all the biocomposites. Upon close examination, there was only a marginal change ($\Delta T < 0.5$ °C) in T_{m1} and T_{m2} of OPMF/PBS with the introduction of 10, 30, and 50 wt% OPMF relative to that of neat

PBS. However, the introduction of 70 wt% OPMF further reduced (ΔT around 1 to 3 °C) the T_{m1} and T_{m2} of PBS. This was clearly demonstrated by the shifting of the endothermic peaks to lower temperatures as can be seen in Fig. 6. A similar trend was also observed for ΔH_m . The ΔH_m of neat PBS was found to be 57.7 J/g, and decreased from 49.1 to 10.9 J/g as the content of OPMF increased from 10 to 70 wt%. The results showed OPMF/PBS biocomposites absorbed less heat energy during melting. The decrease in ΔH_m also led to a decrease in χ_c of PBS at all fiber contents. The initial χ_c of neat PBS was found to be 52.3%. Upon introduction of 10, 30, 50, and 70 wt% OPMF into the PBS, the χ_c decreased to 49.4, 46.9, 40.3, and 32.9%, respectively. The decrease in χ_c of biocomposites can be related to the low χ_c of OPMF, which was reported to be around 33.0% (Then *et al.* 2014b). Apart from that, the presence of OPMF could also disturb the chain arrangement in PBS, thereby decreasing the χ_c of biocomposites.

In the meantime, the crystallization peak (Fig. 7) of PBS appeared to be shifted toward lower temperatures as the content of OPMF increased. The T_c of neat PBS was 89.5 °C and decreased to 89.1, 88.6, 87.7, and 84.9 °C after introduction of 10, 30, 50, and 70 wt% OPMF, respectively. A similar trend was also observed for ΔH_c . The decrease in T_c and ΔH_c resulted from the increase in viscosity of the biocomposite due to the confinement of polymer chains by OPMF, which can hinder the migration and diffusion of PBS molecular chains toward the surface during the crystallization process (Terzopoulou *et al.* 2014).

Thermal Stability

Thermogravimetric analysis was performed in order to study the influence of OPMF and its content on the thermal stability of OPMF/PBS biocomposites. The weight loss and derivative weight loss as a function of temperature for OPMF, PBS, and their biocomposites are illustrated in Figs. 8 and 9, respectively. These thermograms can provide information about the nature and extent of degradation of the biocomposite materials, such as the temperatures where moisture is volatilized from the material, as well as the weight lost due to the thermal degradation process. The detailed evaluations of the thermograms are presented in Tables 4 and 5.

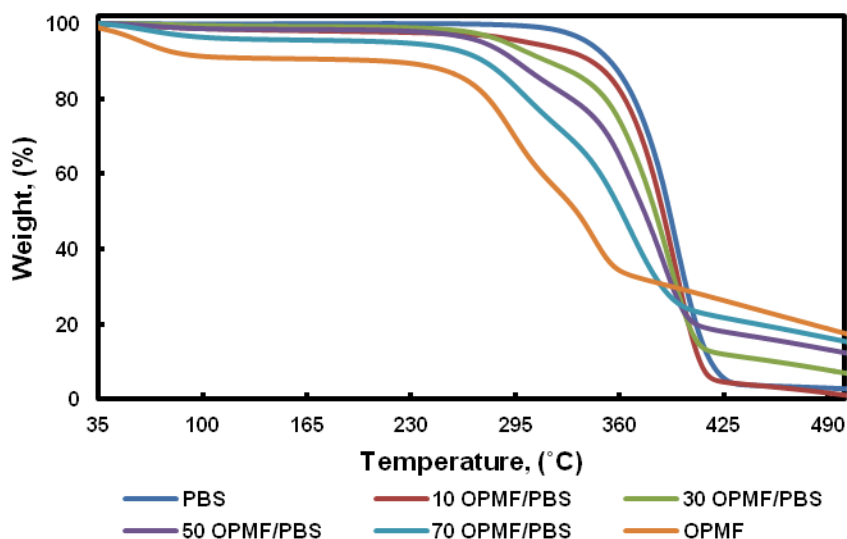


Fig. 8. TG thermograms of OPMF, PBS, and their biocomposites of various OPMF content

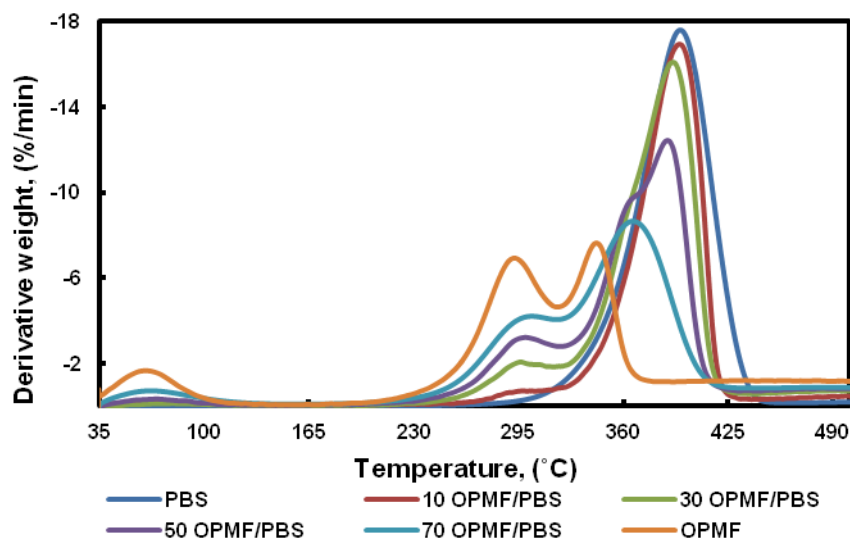


Fig. 9. DTG thermograms of OPMF, PBS, and their biocomposites of various OPMF content

As can be seen in Figs. 8 and 9, PBS showed a single degradation step over the temperature range of this study, indicating that the thermal degradation of PBS consisted of one step weight loss in accordance with the random chain scission reaction. Meanwhile, OPMF showed three degradation steps due to the sequential degradation of fiber components *i.e.*, cellulose, hemicellulose, and lignin. The initial weight loss (35 to 160 °C) is attributed to the evaporation of the water from the fiber followed by hemicellulose and cellulose degradation in the temperature range of 160 to 315 and 315 to 500 °C, respectively (Then *et al.* 2014b). The degradation of lignin occurs slowly within the whole temperature range (160 to 500 °C), owing to its complex structure. This result clearly demonstrated that the thermal stability of OPMF was relatively low in comparison to that of neat PBS.

Table 4. Thermal Degradation Temperatures of PBS and Biocomposites at 5, 10, and 50% Weight Loss and Their Residue at 500 °C

Sample	Temperature °C			Residue at 500 °C, (%)
	$T_{5\%}$	$T_{10\%}$	$T_{50\%}$	
PBS	340.6	354.3	391.2	2.77
10 OPMF/PBS	301.4	341.9	386.7	1.03
30 OPMF/PBS	289.3	315.4	382.2	7.19
50 OPMF/PBS	274.7	295.4	375.4	12.42
70 OPMF/PBS	89.3	254.8	359.9	13.88
OPMF	63.5	215.4	333.0	17.60

Generally, the TG and DTG curves of the OPMF/PBS biocomposites of different weight percentages of OPMF fell between those of PBS and OPMF, depending on the OPMF content. It is apparent that the thermal stability of PBS decreased upon the introduction of OPMF. A similar result was also reported by Nam *et al.* (2011) for coir/PBS biocomposites. The decrease in thermal stability of OPMF/PBS biocomposites could have resulted from the lower onset degradation temperature (~ 160 °C) of OPMF relative to that of PBS (~ 300 °C). The thermal stability of the biocomposites could also be determined by the temperature at which 10% weight loss ($T_{10\%}$) occurred. As shown in

Table 4, the $T_{10\%}$ of neat PBS appeared to be 354.3 °C and decreased to 341.9, 315.4, 295.4, and 254.8 °C for 10, 30, 50, and 70 wt% OPMF, respectively. From the above results, it is clear that the thermal stability of biocomposites was affected by the content of OPMF.

Apart from that, the introduction of OPMF into PBS increased the char formation of the biocomposites, as indicated by the increase in residue at 500 °C. The residue of PBS at 500 °C was 2.77%, and it increased to 7.19, 12.42, and 13.88% for biocomposites filled with 30, 50, and 70 wt% OPMF, respectively. The increase in residues of biocomposites as fiber content increased was related to the residue of OPMF being relatively higher (17.60%) than that of PBS (2.77%) at 500 °C. This result revealed that the presence of OPMF could effectively raise the char yield of the materials. As reported by Shih *et al.* (2004), the char yield is directly correlated to the potency of flame retardation for the materials. The increase in residue content can limit the production of combustible gases and subsequently decrease the exothermicity of the pyrolysis reaction as well as inhibit the thermal conductivity of the burning materials (Pearce and Leipins 1975). This implies that the introduction of OPMF into the PBS may have increased the flame retardancy of PBS.

As can be seen in Fig. 9 and Table 5, the neat PBS showed a single derivative peak with a maximum rate of weight loss (T_{max}) at 395.3 °C. Meanwhile, OPMF showed three derivative peaks with T_{max} values of 63.3, 292.3, and 343.8 °C corresponding to the maximum rate of weight loss due to moisture evaporation, hemicellulose, and cellulose degradation, respectively. For biocomposites, three derivative peaks could be seen in their DTG thermograms. The first and second derivative peaks that appeared in the DTG thermograms of the biocomposites are attributed to the evaporation of moisture and the degradation of hemicellulose from fiber, respectively. At a temperature range of 315 to 500 °C, the thermal degradation of PBS overlapped with those of cellulose and lignin degradations in OPMF; thereby, only one derivative peak is observed. Generally, the T_{max} of the biocomposites at a particular temperature region increased with increasing of PBS content. This may have contributed to the relatively high thermal stability of PBS, which could provide a shielding effect to the degradation process of OPMF and subsequently increased the T_{max} .

Table 5. Temperature at Maximum Rate of Degradation (T_{max}) and Weight Loss of PBS and Its Biocomposites at Different Degradation Stage

Sample	35-160 °C		160-315 °C		315-500 °C	
	T_{max} (°C)	Weight loss (%)	T_{max} (°C)	Weight loss (%)	T_{max} (°C)	Weight loss (%)
PBS	-	-	-	1.20	395.3	96.03
10 OPMF/PBS	70.7	0.73	297.2	5.41	394.4	92.83
30 OPMF/PBS	69.6	2.01	297.7	7.92	391.6	82.88
50 OPMF/PBS	68.9	1.59	297.8	14.29	387.8	71.70
70 OPMF/PBS	65.6	7.07	295.2	18.02	354.4	61.03
OPMF	63.3	9.33	292.3	32.20	343.8	40.87

It can be noted that the major weight losses (96.03%) of PBS were found in the temperature range of 315 to 500 °C, and there was a very minor weight loss of 1.20% in the temperature range of 160 to 315 °C. On the other hand, OPMF showed major weight losses of 32.20 and 40.87% in a temperature range of 160 to 315 °C and 315 to 500 °C,

respectively. For biocomposites, weight losses in the temperature ranges of 35 to 160 °C and 160 to 315 °C decreased with increasing PBS content. This was attributed to the shielding effect of PBS that may have inhibited or delayed the thermal degradation of OPMF. Meanwhile, the weight loss of biocomposites in the temperature range of 315 to 500 °C increased with increasing content of PBS. This was attributed to the increase in content of PBS, which showed major weight loss in this temperature range.

Dimensional Stability

The water absorption and thickness swelling of neat PBS and the biocomposites of various percentages OPMF after 24 h of immersion in distilled water are presented in Fig. 10. It can be clearly seen that the water absorption and thickness swelling of biocomposites were directly proportional to the fiber content.

The neat PBS absorbed very little water (<1%) because of its hydrophobic nature. The dimensional stability of the biocomposites was noted to be negatively affected by the presence of OPMF content. For instance, the water absorption of the OPMF/PBS biocomposites increased from 0.93% to 2.53, 6.51, 11.41, and 22.20% as fiber content increased to 10, 30, 50, and 70 wt%, respectively. This can be explained by the fact that OPMF is hydrophilic in nature; therefore, biocomposites containing a higher content of OPMF will have more water absorption sites and thus an increased rate of water absorption. Also, the thickness swelling of the biocomposites followed a similar trend as water absorption. The neat PBS showed a low thickness swelling of 0.72%. The values increased to 0.85, 2.98, 4.19, and 10.81% after introduction of 10, 30, 50, and 70 wt% OPMF into the PBS, respectively. According to Then *et al.* (2014a, 2015a), the degree of thickness swelling is proportional to the amount of water absorbed. Therefore, greater thickness swelling at high fiber content was ascribed to the high water absorption rate.

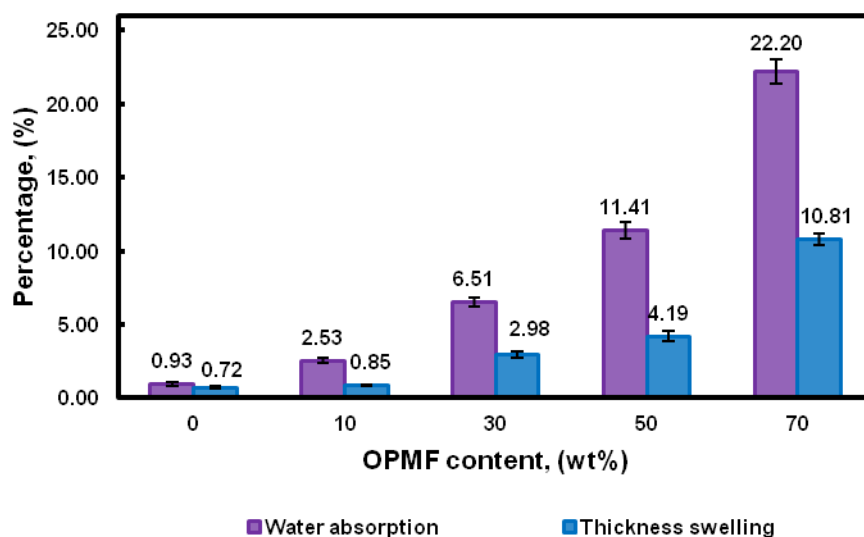


Fig. 10. Water absorption and thickness swelling of neat PBS and its biocomposites of various OPMF content

Biodegradability

The introduction of OPMF into PBS could result in fully biodegradable biocomposite materials due to the fact that both of the components are biodegradable. It is well known that the natural soil degradation test is a slow process. Nevertheless, it is

noteworthy that the soil degradation test could reflect real-life conditions better than any other tests (Kim *et al.* 2005b). In this work, the biodegradability of PBS and its biocomposites was studied by measuring their weight loss in a natural soil degradation test lasting five months, and their results are presented in Fig. 11. Generally, both PBS and OPMF/PBS biocomposites lost weight after the natural soil degradation test. Nevertheless, OPMF/PBS biocomposites showed a higher percentage loss in weight relative to that of neat PBS.

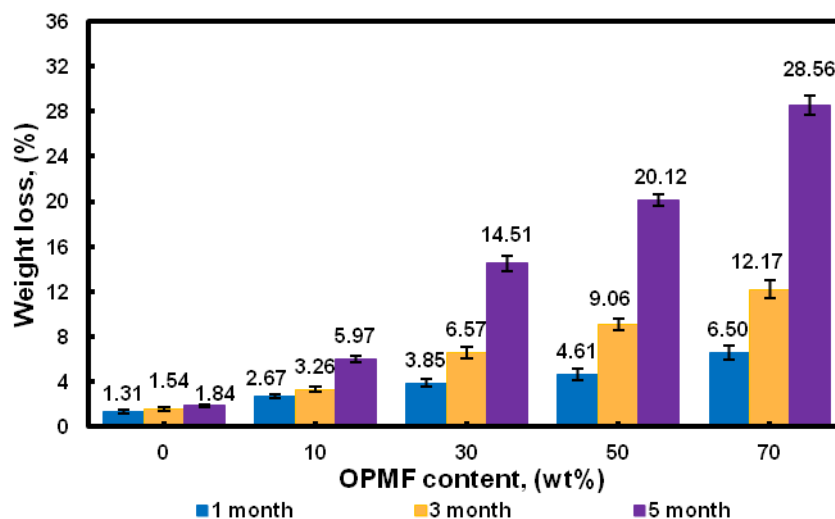


Fig. 11. Weight loss of PBS and its biocomposites of various OPMF content under natural soil buried test

As can be seen in Fig. 11, neat PBS lost a relatively low percentage of weight over the degradation period. The PBS lost only 1.84% of its initial weight after undergoing five months of natural soil degradation. The low biodegradation rate of PBS was explained by its relatively high crystallinity (shown in DSC analysis) and water resistance, which inhibited the biodegradation process. In the meantime, the presence of OPMF promoted the biodegradability of PBS as indicated by a relatively high percentage weight loss of the OPMF/PBS biocomposites over the degradation period. For instance, after five months of the degradation test, the percentage weight loss of neat PBS increased from 1.84% to 5.97, 14.51, 20.12, and 28.56% for biocomposites of 10, 30, 50, and 70 wt% OPMF, respectively. Furthermore, it can be seen that as the OPMF content increased, the percentage weight loss also increased. This result indicated that the presence of OPMF accelerated the degradation process of PBS, mainly because of the increased polymer surface created after OPMF consumption by microorganisms (Singh *et al.* 2003). Additionally, the decrease in crystallinity of PBS after the introduction of OPMF, as discussed previously in the DSC analysis, may also facilitate the biodegradation process, as a less crystalline structure is more accessible to the attack of microorganisms.

Initially, the percentage weight loss for both PBS and its biocomposites was relatively low. This can be explained by the fact that during the initial natural soil degradation process, both the neat PBS and its biocomposites were in the process of absorbing water from the surrounding soil, and their individual components swelled to promote the growth of microorganisms as well as to initiate the hydrolysis reaction. Within this period, both PBS and its biocomposites showed low percentages of weight

loss ($< 7\%$), yet biocomposites showed relatively higher percentages of weight loss than did neat PBS. It seems that the presence of fiber promoted water absorption and the growth of microorganisms on the material's surface and subsequently increased the biodegradation rate of the biocomposites. As the OPMF content increased, both water absorption and thickness swelling increased too; thereby, biocomposites of higher OPMF content showed greater percentage weight loss during a particular period. This is in line with the results discussed previously on the dimensional stability of the biocomposites. This also explains the reason why hydrophobic PBS had a low biodegradation rate. As the degradation period increased, more and more microorganisms grew on the surface of the materials, thereby accelerating their degradation rate as indicated by increasing percentages of weight lost with the prolonged degradation period. For example, the initial percentage weight loss of 70 OPMF/PBS biocomposite was found to be 6.50%, and it increased substantially to 12.17 and 28.56% after undergoing the natural soil degradation process for three and five months, respectively. This result was in agreement with the previous report (Terzopoulou *et al.* 2014).

Surface Morphology

To visualize the morphological changes that occurred due to the natural soil degradation process, scanning electron micrographs of neat PBS and its biocomposite of 70 wt% OPMF before and after soil burial were taken. It was clear that the neat PBS exhibited a relatively smooth and even surface before the natural soil degradation test, as shown in Fig. 12a.

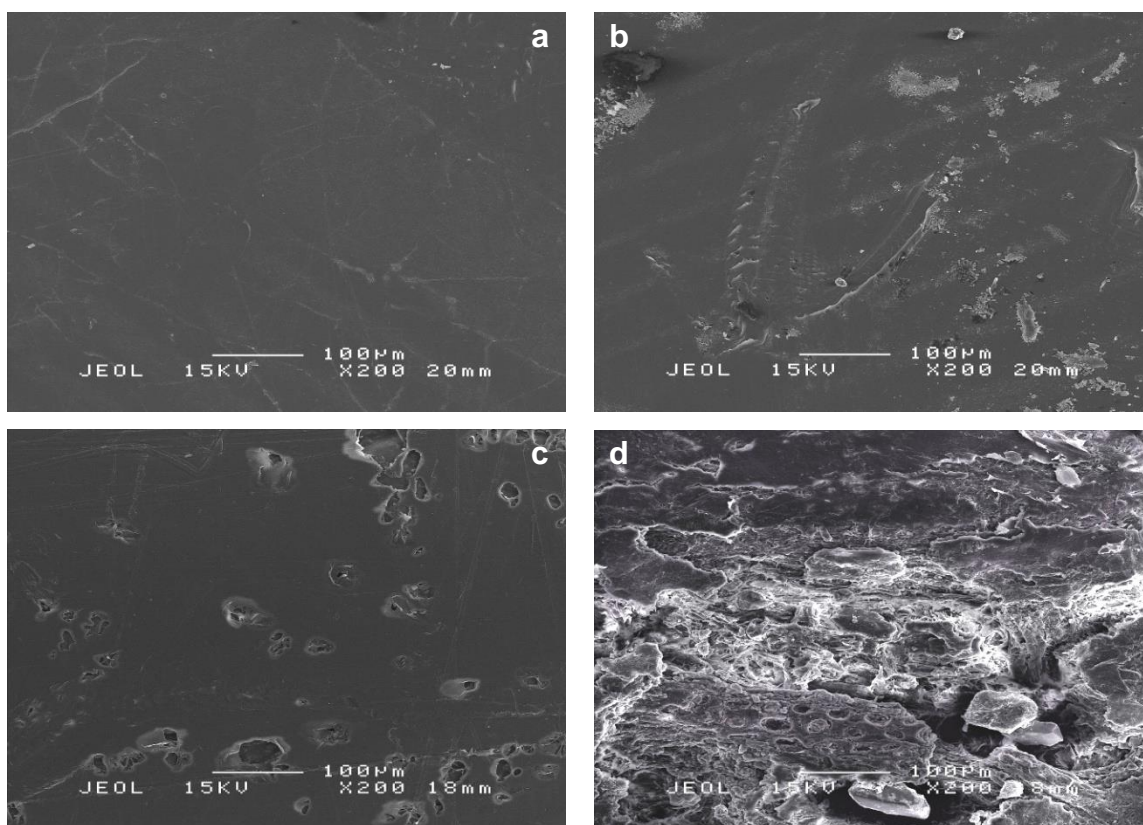


Fig. 12. Scanning electron micrographs of neat PBS (a and b) and biocomposites at 70 wt% OPMF (c and d) before (left) and after (right) soil burial test

Conversely, after five months of degradation, surface erosion as well as the presence of a number of voids can be clearly seen on the surface of PBS (Fig. 12b), indicating that the surface of PBS was partially consumed by the microorganisms in the soil environment (Kim *et al.* 2005b). Figure 12c shows the surface of OPMF/PBS biocomposite at 70 wt% fiber content before the degradation test. Its surface appeared to be relatively smooth with the presence of number of voids. After five months of degradation more numerous surface irregularities could be seen relative to that of neat PBS. Fibers also appeared more exposed due to the loss of the PBS layer that was consumed by microorganisms. This observation confirms that fibers had great influence on the microbial attack in OPMF/PBS biocomposite. A similar observation was also reported by Kim *et al.* (2006) on the bio-flour filled poly(butylene succinate) biocomposites. The SEM micrographs confirmed the results from the biodegradability test.

CONCLUSIONS

1. The storage and loss moduli of PBS were improved with the presence of OPMF. The damping properties of biocomposites decreased with increasing fiber content.
2. The introduction of OPMF into PBS reduced the melting and crystallization temperatures of PBS as well as its crystallinity.
3. The thermal stability of OPMF/PBS biocomposites was at an intermediate level between PBS and OPMF, depending on the OPMF content.
4. The water absorption, thickness swelling, and biodegradability of PBS increased with OPMF content.

ACKNOWLEDGMENTS

The first author would like to acknowledge Ministry of Education, Malaysia, for the provision of a MyPhD scholarship. The authors would also like to thank the Exploratory Research Grant Scheme (ERGS) from the Ministry of Higher Education (MOHE), Malaysia, for their financial support.

REFERENCES CITED

- Abdul Razak, N. I., Ibrahim, N. A., Zainuddin, N., Rayung, M., and Saad, W. Z. (2014). "The influence of chemical surface modification of kenaf fiber using hydrogen peroxide on the mechanical properties of biodegradable kenaf fiber/poly(lactic acid) composites," *Molecules* 19(3), 2957-2968. DOI: 10.3390/molecules19032957
- ASTM. (2008). "ASTM D3418- Standard test method for transition temperatures and enthalpies of fusion and crystallization of polymers by differential scanning calorimetry," *Book of Standards Volume: 08.02*, ASTM, West Conshohocken, PA.

- ASTM. (2009). "ASTM D5023- Standard test method for plastics: dynamic mechanical properties: in flexure (three-point bending)," *Book of Standards Volume: 08.02*, ASTM, West Conshohocken, PA.
- ASTM. (2005). "ASTM D570- Standard test method for water absorption of plastics," *Book of Standards Volume: 08.01*, ASTM, West Conshohocken, PA.
- Azizi Samir, M. A. S., Allioin, F., and Dufresne, A. (2005). "Review of recent research into cellulosic whiskers, their properties and their application in nanocomposite field," *Biomacromolecules* 6(2), 612-626. DOI: 10.1021/bm0493685
- Bikiaris, D. N., Papageorgiou, G. Z., and Achilias, D. S. (2006). "Synthesis and comparative biodegradability studies of three poly(alkylene succinate)s," *Polymer Degradation and Stability* 91(1), 31-43. DOI:10.1016/j.polymdegradstab.2005.04.030
- EN 317. (2003). "- Particleboard and fiberboards; determination of swelling in thickness after immersion in water," European Committee for Standardization, London.
- Eng, C. C., Ibrahim, N. A., Zainuddin, N., Ariffin, H., Wan Yunus, W. M. Z., and Then, Y. Y. (2014). "Enhancement of mechanical and dynamic mechanical properties of hydrophilic nanoclay reinforced polylactic acid/polycaprolactone/oil palm mesocarp fiber hybrid composites," *International Journal of Polymer Science* 2014, 1-8. DOI:10.1155/2014/715801
- Harris, B., Braddel, O., Almond, D., Lefebure, C., and Verbic, J. (1993). "Study of carbon fiber surface treatment by dynamic mechanical analysis," *Journal of Materials Science* 28(12), 3353-3366. DOI: 10.1007/BF00354259
- Joseph, P.V., Mathew, G., Joseph, K., Groeninckx, G., and Thomas, S. (2003). "Dynamic mechanical properties of short sisal fibre reinforced polypropylene composites," *Composites Part A: Applied Science and Manufacturing* 34(3), 275-290. DOI: 10.1016/S1359-835X(02)00020-9
- Kim, H. S., Kim, H. J., Lee, J. W., and Choi, I. G. (2006). "Biodegradability of bio-flour filled biodegradable poly(butylene succinate) bio-composites in natural and compost soil," *Polymer Degradation and Stability* 91(5), 1117-1127. DOI: 10.1016/j.polymdegradstab.2005.07.002
- Kim, H. S., Yang, H. S., Kim, H. J., Lee, B. J., and Hwang, T. S. (2005a). "Thermal properties of agro-flour-filled biodegradable polymer bio-composites," *Journal of Thermal Analysis and Calorimetry* 81(2), 299-306. DOI: 10.1007/s10973-005-0782-7
- Kim, H. S., Yang, H. S., and Kim, H. J. (2005b). "Biodegradability and mechanical properties of agro-flour filled polybutylene succinate bio-composites," *Journal of Applied Polymer Science* 97(4), 1513-1521. DOI: 10.1002/app.21905
- Mohanty, A. K., Misra, M., and Drazel, L. T. (2002). "Sustainable bio-composites from renewable resources: opportunities and challenges in the green materials world," *Journal of Polymers and the Environment* 10(1-2), 19-26. DOI: 10.1023/A:1021013921916
- Nam, T. H., Ogihara, S., Nakatani, H., Kobayashi, S., and Song, J. I. (2012). "Mechanical and thermal properties and water absorption of jute fiber reinforced poly(butylene succinate) biodegradable composites," *Advanced Composite Materials* 21(3), 241-258. DOI: 10.1080/09243046.2012.723362
- Nam, T. H., Ogihara, S., Tung, N. H., and Kobayashi, S. (2011). "Effect of alkali treatment on interfacial and mechanical properties of coir fiber reinforced poly(butylene succinate) biodegradable composites," *Composites Part B: Engineering* 42(6), 1648-1656. DOI: 10.1016/j.compositesb.2011.04.001

- Pearce, E. M., and Leipins, R. (1975). "Flame retardants," *Environmental Health Perspectives* 11, 59-69.
- Pothan, L. A., Oommen, Z., and Thomas, S. (2003). "Dynamic mechanical analysis of banana fiber reinforced polyester composites," *Composites Science and Technology* 63(2), 283-293. DOI: 10.1016/S0266-3538(02)00254-3
- Rayung, M., Ibrahim, N. A., Zainuddin, N., Saad, W. Z., Abdul Razak, N. I., and Chieng, B. W. (2014). "The effect of fiber bleaching treatment on the properties of poly(lactic acid)/oil palm empty fruit bunch fiber composites," *International Journal of Molecular Sciences* 15(8), 14728-14742. DOI: 10.3390/ijms150814728
- Rezaei, F., Yunus, R., and Ibrahim, N. A. (2009). "Effect of fiber length on thermomechanical properties of short carbon fiber reinforced polypropylene composites," *Materials and Design* 30(2), 260-263. DOI: 10.1016/j.matdes.2008.05.005
- Shih, Y. F., Wang, Y. T., Jeng, R. J., and Wei, K. M. (2004). "Expandable graphite systems for phosphorus-containing unsaturated polyesters. I. Enhanced thermal properties and flame retardancy," *Polymer Degradation and Stability* 86, 339-348. DOI: 10.1016/j.polymdegradstab.2004.04.020
- Shinoj, S., Panigrahi, S., and Visvanathan, R. (2010). "Water absorption pattern and dimensional stability of oil palm fiber-linear low density polyethylene composites," *Journal of Applied Polymer Science* 117(2), 1064-1075. DOI: 10.1002/app.31765
- Shinoj, S., Visvanathan, R., Panigrahi, S., and Kochubabu, M. (2011a). "Oil palm fiber (OPF) and its composites: A review," *Industrial Crops and Products* 33(1), 7-22. DOI: 10.1016/j.indcrop.2010.09.009
- Shinoj, S., Visvanathan, R., Panigrahi, S., and Varadharaju N. (2011b). "Dynamic mechanical properties of oil palm fibre (OPF)-linear low density polyethylene (LLDPE) biocomposites and study of fibre-matrix interactions," *Biosystems Engineering* 109(2), 99-107. DOI: 10.1016/j.biosystemseng.2011.02.006
- Singh, R. P., Pandey, J. K., Rutot, D., Degee, P. H., and Dubois, P. H. (2003). "Biodegradation of poly(ϵ -caprolactone)/starch blends and composites in composting and culture environment: The effect of compatibilization on the inherent biodegradability of the host polymer," *Carbohydrate Research* 338(17), 1759-1769. DOI: 10.1016/S0008-6215(03)00236-2
- Sreekala, M. S., Kumaran, M. G., and Thomas, S. (1997). "Oil palm fibers: Morphology, chemical composition, surface modification, and mechanical properties," *Journal of Applied Polymer Science* 66(5), 821-835. DOI: 10.1002/(SICI)1097-4628(19971031)66:5<821::AID-APP2>3.0.CO;2-X
- Tan, B., Qu, J. P., Liu, L. M., Feng, Y. H., Hu, S. X., and Yin, X. C. (2011). "Non-isothermal crystallization kinetics and dynamic mechanical thermal properties of poly(butylene succinate) composites reinforced with cotton stalk bast fibers," *Thermochimica Acta* 525(1-2), 141-149. DOI: 10.1016/j.tca.2011.08.003
- Teh, C. C., Ibrahim, N. A., and Wan Yunus, W. M. Z. (2013). "Response surface methodology for the optimization and characterization of oil palm mesocarp fiber-graft-poly(butyl acrylate)," *BioResources* 8(4), 5244-5260. DOI: 10.15376/biores.8.4.5244-5260
- Terzopoulou, Z. N., Papageorgiou, G. Z., Papadopoulou, E., Athanassiadou, E., Reinders, M., and Bikiaris, D. N. (2014). "Development and study of fully biodegradable composite materials based on poly(butylene succinate) and hemp fibers or hemp shives," *Polymer Composites* [Online first]. DOI: 10.1002/pc.23194

- Then, Y. Y., Ibrahim, N. A., Zainuddin, N., Ariffin, H., and Wan Yunus, W. M. Z. (2013). "Oil palm mesocarp fiber as new lignocellulosic material for fabrication of polymer/fiber biocomposites," *International Journal of Polymer Science* 2013, 1-7. DOI: 10.1155/2013/797452
- Then, Y. Y., Ibrahim, N. A., Zainuddin, N., Ariffin, H., Wan Yunus, W. M. Z., and Chieng, B. W. (2014a). "The influence of green surface modification of oil palm mesocarp fiber by superheated steam on the mechanical properties and dimensional stability of oil palm mesocarp fiber/poly(butylene succinate) biocomposite," *International Journal of Molecular Sciences* 15(9), 15344-15357. DOI: 10.3390/ijms150915344
- Then, Y. Y., Ibrahim, N. A., Zainuddin, N., Ariffin, H., Wan Yunus, W. M. Z., and Chieng, B. W. (2014b). "Surface modifications of oil palm mesocarp fiber by superheated steam, alkali, and superheated steam-alkali for biocomposite applications," *BioResources* 9(4), 7467-7483. DOI: 10.15376/biores.9.4.7467-7483
- Then, Y. Y., Ibrahim, N. A., Zainuddin, N., Ariffin, H., Wan Yunus, W. M. Z., and Chieng, B. W. (2015a). "Static mechanical, interfacial, and water absorption behaviors of alkali treated oil palm mesocarp fiber reinforced poly(butylene succinate) biocomposites," *BioResources* 10(1), 123-136. DOI:10.15376/biores.10.1.123-136
- Then, Y. Y., Ibrahim, N. A., Zainuddin, N., Chieng, B. W., Ariffin, H., and Wan Yunus, W. M. Z. (2015b). "Influence of alkaline-peroxide treatment of fiber on the mechanical properties of oil palm mesocarp fiber/poly(butylene succinate) biocomposite," *BioResources* 10(1), 1730-1746. DOI: 10.15376/biores.10.1.1730-1746
- Xu, J., and Guo, B. H. (2010). "Poly(butylene succinate) and its copolymers: Research, development and industrialization," *Biotechnology Journal* 5(11), 1149-1163. DOI: 10.1002/biot.201000136
- Yasuniwa, M., and Satou T. (2002). "Multiple melting behavior of poly(butylene succinate). I. Thermal analysis of melt-crystallized samples," *Journal of Polymer Science Part B: Polymer Physics* 40(21), 2411-2420. DOI: 10.1002/polb.10298
- Zhang, K., Mohanty, A. K., and Misra, M. (2012). "Fully biodegradable and biorenewable ternary blends from polylactide, poly(3-hydroxybutyrate-co-hydroxyvalerate) and poly(butylene succinate) with balanced properties," *ACS Applied Materials and Interfaces* 4(6), 3091-3101. DOI: 10.1021/am3004522
- Zhao, P., Liu, W. Q., Wu, Q. S., and Ren, J. (2010). "Preparation, mechanical, and thermal properties of biodegradable polyesters/poly(lactic acid) blends," *Journal of Nanomaterials* 2010, 1-8. DOI:10.1155/2010/287082

Article submitted: November 19, 2014; Peer review completed: March 21, 2015; Revised version received and accepted: March 23, 2015; Published: March 30, 2015.
DOI: 10.15376/biores.10.2.2949-2968